IMAGING SUBSURFACE DEFECTS USING SQUID MAGNETOMETERS

Yu Pei Ma and John P. Wikswo, Jr.
Electromagnetics Laboratory
Department of Physics and Astronomy
Vanderbilt University, Nashville, TN 37235

INTRODUCTION

Over the last several years, SQUID magnetometers have been utilized for detection of defects in metal structures by measuring the magnetic field produced by injected current or permanent magnetization [1,2,3]. Because the amplitude of the output signal from the SQUID magnetometer is independent of the frequency of the magnetic field to be measured, SQUIDs are suitable for dc or low frequency measurements as required for detection of subsurface flaws inside a conductor.

In some conditions, such as a conductor covered by an insulation layer, or a metal structure into which it is difficult to inject a uniform current, an induced eddy current may be used instead of injected current. However, the excitation coils used in most eddy current methods induce a localized eddy current circulating inside the conductor, which produces a large magnetic field in the normal direction. The magnetic signals due to the flaws are difficult to discriminate from the large field background detected by SQUID magnetometer. We have now extended SQUID NDE by utilizing a technique to induce an extended eddy current with a well-defined direction in a planar metal structure or a thin walled tube. Combining this with the injected current method, we have detected both a hidden corrosion area inside an aluminum plate and crack defects adjacent to fasteners in the bottom layer of lap-joint aluminum plates.

EXPERIMENTAL METHODS

Injected Current Method

The injected current method has been used for detection of defects in a conductors. By injecting a spatially uniform current into the conductors, such as a plate [2,3,4] or a thin-walled tube [5], and measuring the normal component of the magnetic field using a SQUID magnetometer, we can determine the dimensions and the location of the defects.

Review of Progress in Quantitative Nondestructive Evaluation, Vol. 12
Edited by D.O. Thompson and D.E. Chimenti, Plenum Press, New York, 1993

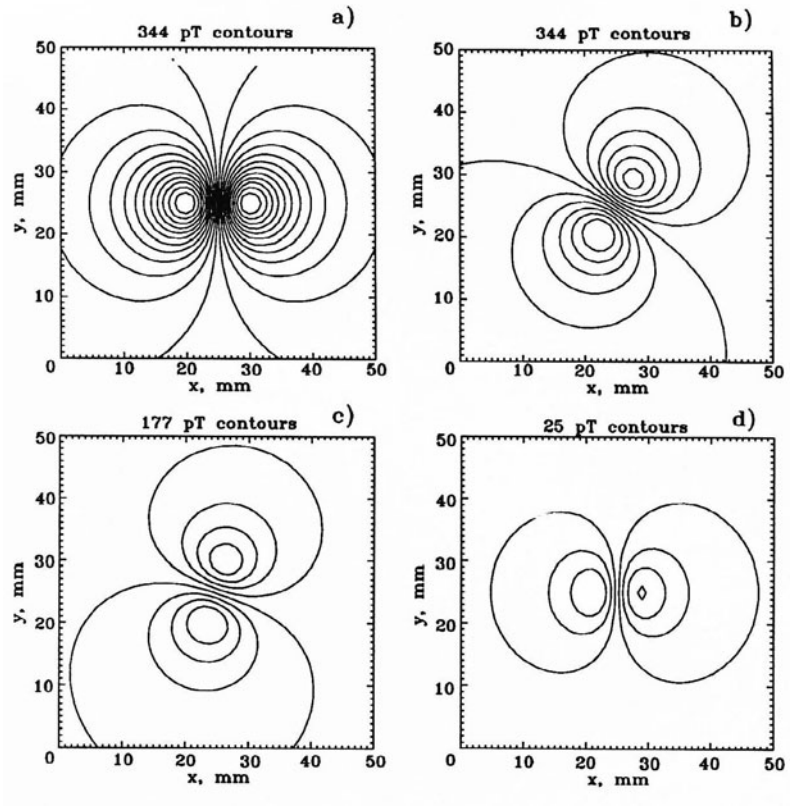

Figure 1. The calculated magnetic field map for a slot with an angle of (a) 90°, (b) 30°, (c) 10°, (d) 0° with respect to the uniform injected current. The slot is 12 mm long by 0.2 mm wide. The injected current density of 20 A/m^2 is in the y direction.

Figure 1 is the calculated contour maps of the normal component of the magnetic field for a 12 mm long slot with angle of 90°, 30°, 10° and 0° with respect to the current injected in the y direction. The lines connecting the maximum and the minimum of the field indicate the orientation of the slot, except for the slot parallel to the current (see Fig. 1(d)) . The amplitude of the signal reduces with the angle because less current is disturbed. For best results, the current should be injected sequentially in two orthogonal directions.

Induced Eddy Current Method

We have used a large thin copper sheet carrying a uniform current for inducing an extended eddy current inside a plate [6]. As shown in Fig. 2(a), the sheet carrying a uniform current in the x direction produces a magnetic field in the y direction, which induces an eddy current in the conducting plate. The sheet may be placed either below or above the test sample. The amplitude of the induced eddy current density is proportional to the frequency of the exciting current, and diminishes with the depth. At the center of the plate the current vanishes. The phase of the eddy current density changes with depth. At the top surface the eddy current is in the direction opposite to the current at the bottom surface.

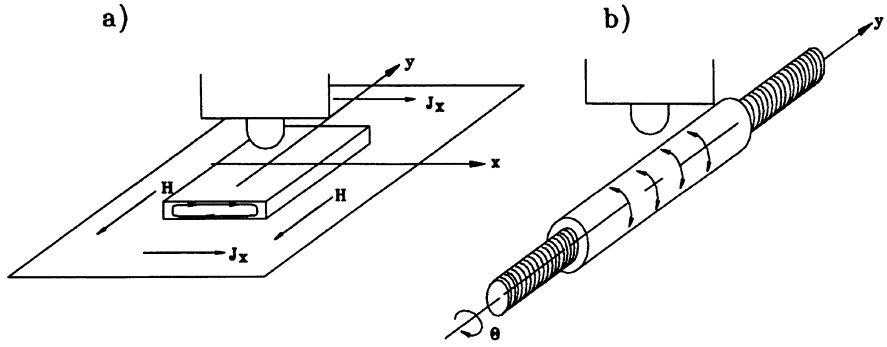

Figure 2. A schematic illustration of the inducers. (a) Parallel plate inducer, (b) Long solenoid inducer.

If both the inducer and the test sample are of infinite extent, the spatially uniform currents in the $x - y$ plane do not produce the magnetic field in the normal direction. Otherwise the edge effect due to the discontinuity of the current density should be considered. The flaw inside the test sample disturbs the current density distribution near the flaw and then produces magnetic field in the normal direction, which may be detected by the SQUID magnetometer. The amplitude and the phase of the magnetic signal due to the flaw are dependent on the dimensions and the depth of the flaw.

For a thin-walled cylindrical conducting tube, a long homogeneous solenoid may induce an azimuthal current in the tube wall (see Fig. 2(b)). In low frequency limit, the skin depth is much larger than the thickness of the wall and the induced current density is uniform with an amplitude that is proportional to the frequency of the exciting current. The phase lag is 90° with respect to the exciting current [6].

EXPERIMENTAL RESULTS

We have detected a corrosion area inside an aluminum plate by injecting low frequency ac current. The plate consists of two layers of 2.5 mm thick plate simulating a lap joint in an aircraft wing surface. A 32 mm diameter corrosion area is located at the center of the bottom surface of the upper plate as shown in Fig. 3. This corrosion area has been measured by profilometer, which suggests a mass loss of 2% . Figure 3(a) is the surface map and Fig. 3(b) is the contour map, made while injecting a 10 Hz 58 mA ac current. The dashed line in Fig. 3(b) indicates the position of the corrosion area relative to the mapping area.

Combining the injected and induced current method, we have detected second-layer cracks immediately adjacent to the fastener. As shown in Fig. 4, the test sample is made of two 7075-T6 aluminum panels bolted together by six aluminum pins and nuts. Each panel is 250 × 100 × 2.4 mm. The crack defects beneath the surface are simulated by saw cut slots in the bottom layer adjacent to the pins A, B and C (see right side of Fig. 4). The pins D, E and F are for reference. The slots are 12 mm long at A and C, and 6 mm long at B. The width of all slots is less than 0.4 mm.

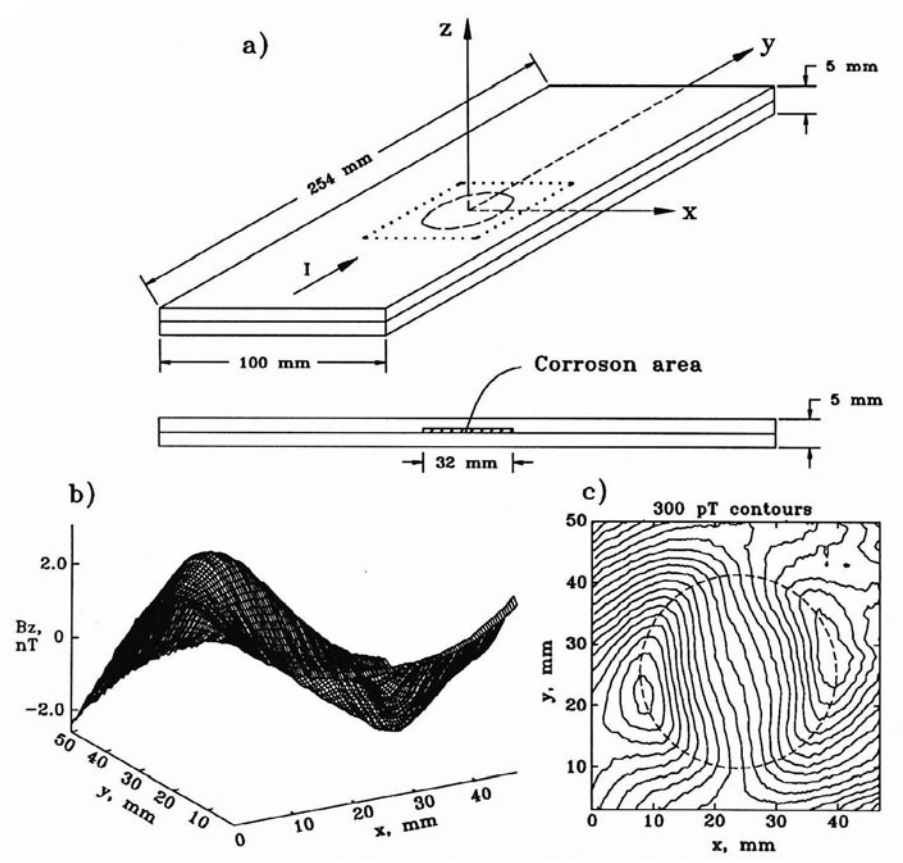

Figure 3. The magnetic field map for a hidden circular corrosion area inside a lap joint of two 2.5 mm thick aluminum plates. The corrosion area, which represented a mass loss of 2%, was located at the center of the bottom surface of the upper plate. A 10 Hz 58 mA ac current was injected into the plate. (a) The surface field map. (b) The contour field map. The contour interval is 300 pT. The dashed line indicates the position of the corrosion area relative to the dotted boundary of the mapping area.

The SQUID pick-up coil is located 3 mm above the head of pins (4.5 mm above the plate). By injecting 47 Hz 30 mA current in the longitudinal direction and mapping the magnetic field around each pin, we have six contour maps as shown in the middle of Fig. 4. Each map is 40 mm $\times$ 40 mm, and the contour interval is 2 nT. Plots of the cross section of the contour maps at the center of the pins in the direction perpendicular to the current are shown at the left of Fig. 4. The current is disturbed by both the pin and slot. The field maps for the three pins without cracks (D, E and F) are almost identical to each other. Obviously, the map for A, which has a slot perpendicular to the current, shows the largest difference from the map of D. The map for C, which has a 12 mm longitudinal slot, does show differences from the map for F, but they are much smaller than A because the slot is almost parallel to the current.

It is difficult to discriminate between the map for B, which has a 6 mm longitudinal slot, and the map for E (see the cross section plots). To detect the longitudinal slots (B and C), the current should be injected in the transverse direction. Instead of injecting current, a copper sheet carrying 340 Hz uniform current was used for inducing the transverse current in the plate. Both the in-phase and quadrature components were recorded. The contour maps for six pins are shown in the Fig. 5, where the contour interval is 180 pT. The maps for pins B and C show the large signal due to the longitudinal slots. The map for pin A also shows the small signal due to the transverse slot. The cross section plots are taken at the center of the pins in longitudinal direction. Comparing Fig. 5 and Fig. 4, the magnetic signal using the induced eddy current is similar to the signal from the injected current method.

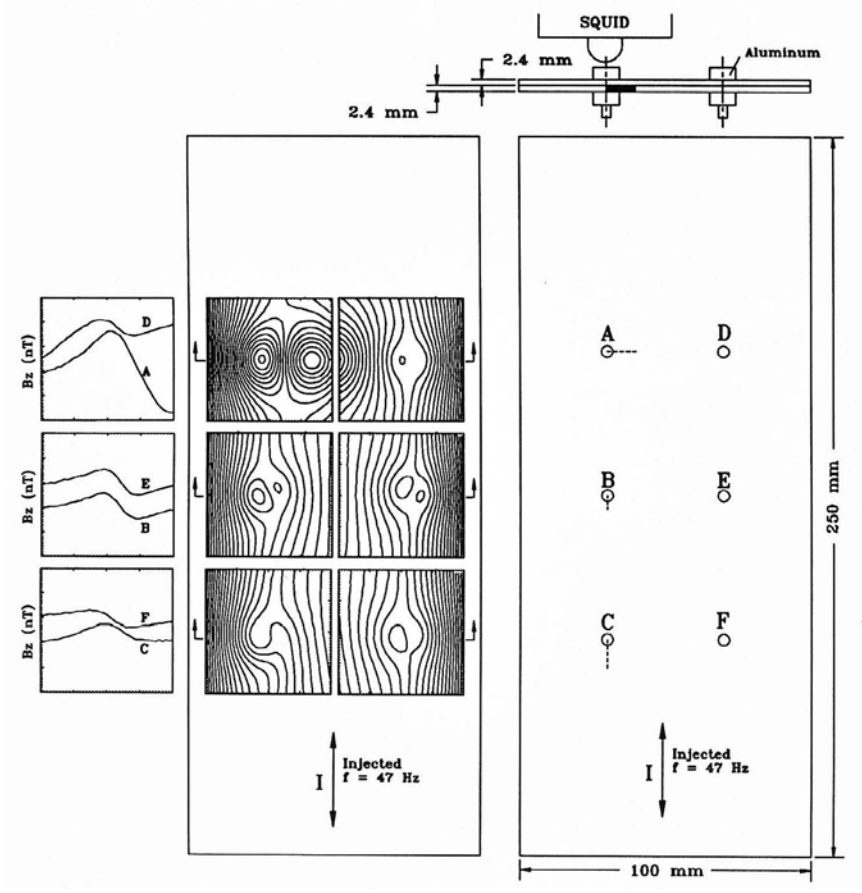

Figure 4. Detection of second-layer cracks by the injected current method. Right: A test sample of two 7075-T6 aluminum panels bolted together by six aluminum pins and nuts. For pins A, B and C, second-layer cracks are simulated by saw cut slots in the bottom layer adjacent to the pins. Middle: Field contour maps when a 47 Hz 30 mA current was injected into the plate in the longitudinal direction. Left: Plots of the cross section of the contour maps taken at the center of the pins in the transverse direction.

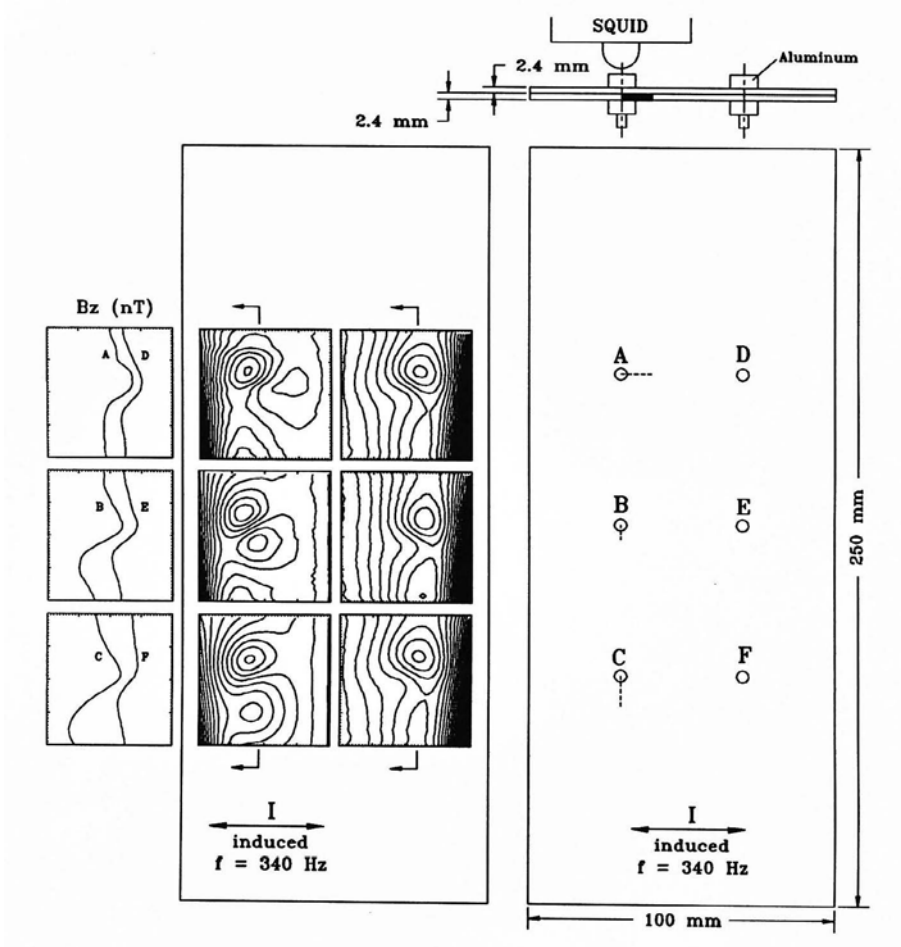

Figure 5. Detection of second-layer cracks by the induced eddy current method. Right: A test sample of two 7075-T6 aluminum panels bolted together by six aluminum pins and nuts. For pins A, B and C, second-layer cracks are simulated by saw cut slots in the bottom layer adjacent to the pins. Middle: Field contour maps when a 340 Hz ac current was induced into the plate in the transverse direction. Left: Plots of the cross section of the contour maps taken at the center of the pins in the longitudinal direction.

CONCLUSIONS

By using low frequency injected current, we have detected a hidden corrosion area with mass loss of 2% inside a lap joint connecting two aluminum plates. In combination with the injected current method, the low frequency eddy current method is capable of discriminating between the current perturbation due to the fasteners and that due to the fasteners with the second-layer cracks. The advantage of the parallel plate and long solenoid inducers is that the magnetic background from

both the inducer and the induced eddy current is minimized. It is especially suitable for a SQUID with a pick-up coil measuring the vertical component. This technique has great potential for detection of subsurface defects in planar metal structures and thin-walled conducting tubes [5].

ACKNOWLEDGEMENTS

This research has been supported by the Electric Power Research Institute, Air Force Office of Scientific Research Grant 87 0337, and Lockheed.

REFERENCES

1. H. Weinstock, "A review of SQUID magnetometry applied to nondestructive evaluation", IEEE Trans. Magnetics, Vol. 27, p3231, (1991).

2. J. P. Wikswo, Jr., J. V. Egeraat, Y. P. Ma, N. G. Sepulveda, D. J. Staton, S. Tan, and R. S. Wijesinghe, "Instrumentation and techniques for high resolution magnetic imaging", *Digital Image Synthesis and Inverse Optics*, A. F. Gmitro, P. S. Idell, and I. J. LaHaie, Eds., SPIE Proceedings, Vol. 1351, p.438 (1990).

3. Y. P. Ma, D. J. Staton, N. G. Sepulveda, and J. P. Wikswo, Jr., "Imaging flaws with a SQUID magnetometer array", *Rev. of Progress in Quantitative Nondestructive Evaluation*, Vol. 10A, p979 (1991).

4. Y. P. Ma and J. P. Wikswo, Jr., "Detection of a deep flaw inside a conductor using a SQUID magnetometer", *Rev. of Progress in Quantitative Nondestructive Evaluation*, Vol. 11A, p1153 (1992).

5. D.C. Hurley, Y.P. Ma, and J.P. Wikswo, Jr.,"A comparison of SQUID imaging techniques for small defects in nonmagnetic tubes", in this volume.

6. Y.P. Ma and J.P. Wikswo, Jr., "Improved techniques for inducing low frequency eddy currents for SQUID-based non-destructive testing" in preparation.